BACKGROUND BIOAEROSOL CHARACTERIZATION

S.G. JENNINGS

(Principal Investigator)
National University of Ireland, Galway

CONTRACT NUMBER: N68171-97-M-5714

Final Report

October 1998

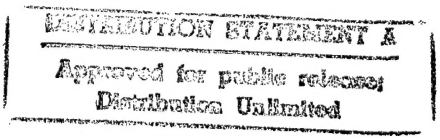

The research reported in this document has been made possible through the support and sponsorship of the U.S. Government through its European Research Office of the U.S. Army. This report is intended only for the internal management use of the Contractor and the U.S Government.

REPORT DOCUMENTATION PAGE

Form Approved
OMB No 0704-0188

1. AGENCY USE ONLY (Leave blank)	2. REPORT DATE	3. REPORT TYPE AND DATES COVERED
	October 1998	Final: August 1997 - October 1998

4. TITLE AND SUBTITLE
Background Bioaerosol Characterization

5. FUNDING NUMBERS
N 68171-97-M-5714

6. AUTHOR(S)
S.G. Jennings and C.M. Kenny

7. PERFORMING ORGANIZATION NAME(S) AND ADDRESS(ES)
University College Galway, Galway, Ireland

8. PERFORMING ORGANIZATION REPORT NUMBER
0004

9. SPONSORING/MONITORING AGENCY NAME(S) AND ADDRESS(ES)
U.S. Army Research, Development and Standardization Group
223 Old Marylebone Road, London NW1 5TH, UK

10. SPONSORING/MONITORING AGENCY REPORT NUMBER

11. SUPPLEMENTARY NOTES
None

12a. DISTRIBUTION/AVAILABILITY STATEMENT
Unlimited

12b. DISTRIBUTION CODE

13. ABSTRACT (Maximum 200 words)

Total aerosol and biological size distributions have been determined for both background (marine) and continental air masses at the Mace Head atmospheric research station on the west coast of Ireland. A combination of meteorological and condensation nuclei number concentration data were used to characterise the air masses. The aerosol size distribution, ranging in diameter from 0.5 μm up to about 50 μm, was obtained from stained samples, using both conventional microscopy and a digital imaging system. In general, lower biological aerosol number concentration levels, by factors from about 2-3 were found for marine background air in comparison with the more polluted continental air. Fluorescence emission spectra were also obtained for both background and polluted conditions.

14. SUBJECT TERMS	15. NUMBER OF PAGES
Background Bioaerosol Size Distribution, Total Background Aerosol Size Distribution, Bioaerosol Fluorescence Spectra	21
	16. PRICE CODE

17. SECURITY CLASSIFICATION OF REPORT	18. SECURITY CLASSIFICATION OF THIS PAGE	19. SECURITY CLASSIFICATION OF ABSTRACT	20. LIMITATION OF ABSTRACT
Unclassified	Unclassified	Unclassified	None

Table of Contents

Figure Captions

Figure 1 (a) - 1 (d) Total and biological aerosol size distribution for the marine periods 07/04/97 and 07/15/97.

Figure 1 (e) - 1 (g) Percentage (%) of biological, non-biological and transparent particles to total aerosol particles for the marine periods 07/04/97 and 07/15/97.

Figure 2 (a) - 2 (h) Total and biological aerosol size distribution for marine and continental periods during the sampling period 07/31/97 - 12/02/97.

Figure 3 (a) - 3 (d) Total and biological aerosol size distribution for the marine and continental periods 03/11/98 and 04/02/98.

Figure 4 (a) - 4 (l) Representative emission fluorescence spectra at selected wavelengths for the marine and continental periods 03/11/98 and 04/02/98.

BACKGROUND BIOAEROSOL CHARACTERIZATION

1. Introduction

Biological particles are an ubiquitous component of the atmospheric aerosol, which is characterized in the atmosphere by a natural background consisting of sulphates, nitrates, sea salt, clay minerals, and other particles (Twomey, 1977; Prospero et al., 1983, 1985; Pinnick et al., 1993). The biological component can amount to between 20-30% of the concentration of total atmospheric particles (Matthias-Maser and Jaenicke, 1995).

It is deemed important to have the capability of distinguishing background bioaerosols which have the distinct potential of interfering with the detection of man-made biological agents. Little information exists on the natural fluorescent background, which is required to determine the effectiveness of bioaerosol detection above the background signal.

The bioaerosol has been largely neglected up to now because it has been believed to be part of the nominally accepted components of the atmospheric aerosol, desert aerosol, remote continental aerosol, marine aerosol, polar aerosol, cloud processed aerosol, biomass burning aerosol and stratospheric aerosol. However the biological aerosol should be considered as an important separate aerosol component. Few size distributions of bioaerosol are yet available; the work of Jaenicke and Matthias (1988) suggest that the biological aerosol can contribute up to 40% of the total aerosol for certain size ranges. It is found by Matthias-Maser (1996) that the biological fraction contains 24% in number concentration and 22% in volume of the total ambient aerosol (urban) population.

Primary bioaerosol particles show a great variation in concentration due to the phenology, meteorological conditions, sampling location and seasonal variations. In a rural location there is an increase in large and giant particles eg. pollens and spores, whereas in urban locations there is a greater abundance of microbial aerosols eg. bacteria. The composition of primary bioaerosol changes in the autumn and winter

when more microorganisms and fragments are present due to decaying vegetation while in spring and summer many pollen species are present during the flowering season (Matthias-Maser and Jaenicke, 1995). A marine environment is a very important source of biological aerosol particles. The 'bubble-burst' mechanism (Blanchard & Sydek, 1972) produces not only sea-salt particles and pure bioaerosol particles but also sea-salt particles that may be biologically contaminated.

2. Aerojet Glass Cyclone Sampler

Effective biological analysis of airborne particles requires samplers operating at a high flow rate and with the capability of concentrating the air particles into a fairly small liquid volume. The Aerojet cyclone high volume sampler currently being used at Mace Head has been proven to be a successful sampler for the collection of bioaerosol material (Griffiths et al., 1997). The collection of bioaerosol particles in a liquid medium allows the potential application of several analysis methods without altering the biological integrity required for their detection.

Operating at a flow rate of 500 l min^{-1}, the Aerojet cyclone has collection fluid continuously sprayed into the sampler inlet, aerosolised biological matter are removed from the airstream mainly through impingement into the liquid film formed along the cyclone walls and then washed off into a collecting reservoir. The sampling efficiency of the cyclone has been characterized in large wind tunnels (Griffiths et al., Upton et al., 1994) and has proved capable of collecting bioaerosol of mean diameter 5-20 μm with efficiencies from 80-100%. The glass cyclone sampler chosen for its good performance has already been successfully used in sampling of biological aerosol at Mace Head (Jennings, 1997). The glass cyclone sampler has a high sampling efficiency (80-100%) which is reasonably independent of wind speed, aerosol diameter and sampler orientation. A representative sample with a good bioefficiency ie. to prevent desiccation and cell damage is required. Cyclones with spray wetters have been found to be gentle with airborne microorganisms and help to maintain cell viability levels.

3. Protocol

The sampling media utilized is a phosphate buffered saline solution which has been filtered through a 0.2 μm pore and autoclaved for 45 minutes at 121°C. The collection bottle, glass cyclone and its associated tubing, hypodermic needle and media carboy are also sterilized prior to sampling. Once a sample has been collected it is refrigerated immediately. A protein dye (Coomassie blue $C_{47}H_{48}N_3O_7S_2Na$) is used to stain biological particles in the bioaerosol sample (Matthias-Maser and Jaenicke, 1994). This is done by adding 0.05 ml of the staining solution per 20 ml of sample. The staining solution reacts with the carboxyl group of a protein and therefore stains the protein-containing or biological particles blue. Non-biologicals are not changed by the stain.

Phosphate buffered gluteraldehyde (GTA) is used at a concentration of 1% to preserve the sample. After a period of two weeks the sample is filtered by vacuum suction onto a 13 mm cellulose nitrate filter (1 μm) placed in a Millipore analytical stainless steel filter holder. The filter is then mounted on a glass slide and when dry covered with immersion oil and a glass cover slip (18 by 18 mm, Chance Propper, No.1). All reagents other than immersion oil are refrigerated (4°C) in the dark and filter sterilized (pore size 0.2 μm) just prior to use. Reagents must be sterile, particle free and at room temperature (21°C) prior to use.

4. Fluorescence Protocol

Total fluorescence of the bioaerosol samples has been determined using a Perkin Elmer LS 50B fluorimeter available at University College Galway. The protocol used for fluorescence measurements at ERDEC by Dr.Steven Christesen and Kate Ka Ong has been adopted for use in this work. Samples collected for total fluorescence measurements are analyzed within 24 hours.

The Perkin Elmer spectrofluorimeter performs the selected emission scans using the following programs:

	Scheme I	Scheme II
Excitation	250-310 nm 4 nm increment	310-530 nm 20 nm increment
Slitwidth	2.5 nm	2.5 nm

Data obtained from the fluorescence measurements generates two dimensional plots of fluorescence intensity as a function of emission and excitation wavelength. Excitation/emission (EEM) spectra were collected for each sample with excitation wavelengths between 250 and 530 nm. The wavelength increment was set at 4 nm for excitation wavelengths from 250 and 310 nm. The excitation wavelength was varied in 20 nm increments from 310-530 nm. The emission wavelength range was dependent on the excitation wavelength, beginning at λ excitation + 5 nm and ending at 2 (λ excitation) - 10 nm, so as to remove Rayleigh scattering and second order fluorescence.

Sterile filtered water was also analyzed using these parameters and the water Raman signal provides a calibration standard for determining the fluorescence cross sections. The ratio of the water Raman peak area to the fluorescence peak area is proportional to the ratio of the water Raman cross section (in cm^2/molecule) to the fluorescence cross section (cm^2/particle). Therefore in each case the water spectrum was subtracted from the sample spectrum and the remaining peak is quantitised using the water Raman peak ratio. The spectra were also corrected for the wavelength dependence of the spectrometer sensitivity; both for emission and excitation.

The relationship between the water Raman peak to the bioaerosol fluorescence signal is given by the following formula:

$$\frac{I_R}{I_F} = \frac{\sigma_R \times C_w}{\sigma_F \times C_B} \qquad (1)$$

or

$$\sigma_F = \frac{\sigma_R \times C_w}{C_B} \times \frac{I_F}{I_R} \qquad (2)$$

where

I_R	=	Integrated water Raman intensity
I_F	=	Integrated fluorescence intensity
σ_R	=	Raman cross section (cm^2/sr/molecule)
σ_F	=	Fluorescence cross section(cm^2/sr/particle)
C_W	=	Water concentration (molecules/ml)
C_B	=	Bioaerosol concentration (particles/ml)

The fluorescence cross section σ_F (Eq.2) is calculable since I_R and I_F are derived from the integration of the Raman and fluorescence spectral signals; and σ_R and C_W are known. The remaining unknown parameter C_B, the bioaerosol concentration has been measured by microscopy and is expressed as particles per milliliter (particles/ml) which represents the total number of biological particles per ml in a liquid sample. An example of the calculation of the number of particles per ml is given in Appendix 1.

5. Microscopy

Microscopy is one of the primary methods used for evaluation of outdoor aerosols. It relies on the existence of characteristics that allow a particle to be recognized visually. Under the light microscope the effects of the protein dye on different particle types can be seen and biological particles can be classified by their characteristic morphology and size. Filters have been examined using a Leitz microscope (Laborlux S), equipped with a 10x ocular lens and an objective lens, Plan 40 (3.5 μm < d < 40 μm) and objective lens, plan 100, oil (1 μm < d < 3.5 μm).. An eyepiece micrometer scale is used in conjunction with a stage micrometer to measure the aerosol particles, resulting in size distributions of total and biological aerosol particles.

The primary disadvantage of using microscopy for routine monitoring of bioaerosols is that it is time and skill intensive. Computerized methods that automate the actual counting procedure allows fast and accurate results to be obtained. Microscopic analysis is transcending into the discipline of analytical imaging, in effect any image obtained microscopically can be digitized. The quality of the digitized image however is still dependent on the clarity of the primary microscopic image. Therefore the most

advanced microscopic applications are only as good as basic light microscopy will allow.

In addition to light microscopic analysis, filters have been examined using a Kontran Elektronic (KS 400) digital imaging system. This system utilizes a Nikon Microphot-FXA video camera attached to a Nikon microscope. The digital imaging system has the capability of sizing particles down to an equivalent diameter of 0.4 μm at x 400 magnification. Therefore from the 07/31/97 onwards, analysis was therefore extended to include particles of equivalent diameter < 1 μm down to 0.4 μm in size (0.4 μm < d < 1 μm).

The precision of counts depends on the number of particles counted. Assuming a Poisson distribution of particles upon the filter, the 95% confidence intervals are approximately twice the square root of the number of particles counted, regardless of the number of grids observed. To reduce the 95% confidence interval to ±10 % of the mean (assuming a Poisson distribution), at least 400 particles per filter are counted. Particles falling within the grid are counted in randomly located fields.

6. Results and Discussion

A combination of meteorological and condensation nuclei (CN) data were used to determine air mass sources. Data include bioaerosol samples from both marine (wind sector 180-300°) and continental air sources (wind sector 45-135°). Two 12 hourly bioaerosol samples collected for marine air conditions at Mace Head during the month of July 1997 have been evaluated into size classes (1 μm < d < 40 μm) and the size distributions of the total aerosol and biological aerosol were obtained. These were plotted as number concentration (dN/dlogD per ml) versus equivalent diameter (μm) and are presented in Figures 1 (a) through 1 (d). The percentages of biological particles to total aerosol particles in the corresponding size classes for both dates are shown in Figures 1 (e); also the percentages of non-biological and transparent particles to total aerosol particles in the corresponding size bins are shown in Figures 1 (f) and 1 (g).

The greatest particle number concentration for total aerosol occurs for the particle diameter interval 1-2 μm for both 07/04/97 and 07/15/97 (Figure 1 (c)). Both samples show a rapid drop in the number of particles per ml at size classes > 3 μm.

Comparing the percentage of biological particles in both samples (Figure 1 (e)) it is apparent that the greatest concentration of biological particles occurs in the particle size range of diameter 1-2 μm. The 07/04/97 data has the highest percentage of biological particles present in this size bin. On the 07/04/97 there are an additional two peaks at size intervals of diameter 14-15 μm and 17-18 μm.

Both samples have the greatest percentage of non-biological particles at particle diameter interval 1-2 μm (Figure 1 (f)). The percentage of transparent particles is also greatest at particle diameter interval 1-2 μm (Figure 1 (g)) for both samples. A second peak occurs on the 07/15/97 in the particle size range 4-5 μm.

Eight 12 hourly bioaerosol samples were collected at Mace Head over the period of July to December 1997. The samples were evaluated into size classes (0.4 μm < d > 51.2 μm) and the size distributions of the total aerosol particles, biological particles non-biological particles and transparent (non-biological) particles were obtained. These were plotted as number concentration (dN/dlogD per ml) versus equivalent diameter (μm) and are presented in Figures 2 (a) through 2 (h).

In general, lower biological aerosol number concentration levels, by factors between about 2-3 were found for marine air as compared to continental air. However, for larger sized particles (diameter ≥ 10 μm), marine air biological particles were generally dominant. The highest concentration of particles occurs during a continental episode on the 10/23/97, on comparing the total aerosol size distributions for the eight sampling periods (Figure 2 (a)). A peak concentration occurs in size intervals of diameter < 3.2 μm for all samples. The highest concentration of particles in the size range of 3.2 μm < d < 6.4 μm occurs during the continental periods of 09/19/97, 10/23/97 and 12/02/97.

The highest concentration of biological particles at the size intervals of diameter 0.4-0.8 μm, 0.8-1.6 μm, and 3.2-6.4 μm occurs during the continental period 10/23/97 (Figure 2 (b)). The peak biological particle concentration at the size interval of diameter 1.6-3.2 μm occurs during the continental period 09/19/97.

Similarly, on comparing the size distribution of black particles for all eight samples (Figure 2 (c)), the highest concentrations also occur during the continental sampling period 10/23/97. The highest concentration of particles occurs in the size ranges < 3.2 μm for all samples. The highest concentration of particles in the size range of 3.2 μm $< d < 6.4$ μm also occurs during the continental periods of 09/19/97, 10/23/97 and 12/02/97.

The continental period 10/23/97 has the highest concentration of transparent particles (Figure 2 (d)). Most samples have a peak concentration occurring in the size interval of diameter 0.8-1.6 μm with the exception of the marine period 08/15/97 which has a peak transparent particle concentration at the size interval 1.6-3.2 μm.

Two 12 hourly bioaerosol samples collected for the marine period 03/11/98 and the continental period 04/02/98 have been evaluated into size classes (0.4 μm $< d <$ 51.2 μm) and the size distributions of the total aerosol and biological aerosol were obtained. These were plotted as number concentration (dN/dlogD per ml) versus equivalent diameter (μm) and are presented in Figures 3 (a) through 3 (d). The continental period 04/02/98 has the highest concentration of particles for particles $>$ 3.2 μm (Figure 3 (c)). The highest concentration of biological particles also occurs during the continental period 04/02/98 (Figure 3 (d)).

Representative fluorescence emission spectra for the sampling periods 03/11/98 and 04/02/98 are shown in Figures 4 (a) through to 4 (l). The emission signal for the continental period is slightly higher than the marine period for all excitation wavelengths.

7. References

Blanchard D.C., Syzdek, L.D. (1972). Concentration of bacteria in jet-drops from bursting bubbles. J. of Geophysical Research, 77, No. 5, 1229-1232.

Griffiths, W.D., Stewart, I.W., Futter, S.J., Upton, S.L., and Mark, D. (1997). The development of sampling methods for the assessment of indoor bioaerosols. J. Aerosol Sci., 28, 437-457.

Jaenicke, R., and Matthias, S. (1988). The primary biogenic fraction of the atmospheric aerosol. In "Aerosols and Climate", P.V. Hobbs and M.P. Mc Cormack (Eds.,), Deepak Publishers, 31-38.

Jennings, S.G. (1997). Characterisation of background biological aerosol.(European Research Office (London) of the U.S. Army). 1st Interim Report Contract No. N 68171-96-C-9124.

Matthias-Maser, S., and Jaenicke, R. (1995). Size distribution of primary biological aerosol particles with radii $r > 0.2$ μm in an urban/rural influenced region. J. Atmos. Res., 39, 279-286.

Matthias-Maser, S. (1996). Primary biological particles: their significance, sources, sampling methods and size distribution in the atmosphere. Submited as a chapter to a book entitled "Atmospheric Particles", John Wiley and Sons Ltd., Chichester, UK.

Pinnick. R.G., Fernandez, G., Martinez-Andazola, E., Hinds, B.D., Hansen, A.D.A., and Fuller, K. (1993). Aerosol in the Arid South-Western United States: Measurements of Mass Loading, Volatility, Size Distribution, Absorption Characteristics, Black Carbon Content and Vertical Structure to 7 Km above sea level. J. Geophys. Res., 98, 2651-2666.

Prospero, J.M., Charlson, R.J., Hohnen, V., Jaenicke, R., Delaney, A.C., Moyers, J., Zoller, W., and Rahn, K. (1983). The atmospheric aerosol system: An overview. Rev. Geophys. Space Phys., 21, 1607-1629.

Prospero, J.M., Savoie, D.L., D.L., Nees, R.T., Duce, R.A., and Merrill, J. (1995). J. Geophys. Res., 90, 10,586-10,596.

Twomey, S. (1977). Atmospheric Aerosols, Elsevier Scientific Publishing Company, New York.

Upton, S.L., Mark, D. Douglass, E.J., and Griffiths, W.D. (1994). The wind tunnel evaluation of the sampling efficiency of three biological aerosol samplers. J. Aerosol Sci., 25, 1493-1501.

Appendix 1 :

Calculations of the number of particles/ml from light microscopy measurements.

$$\text{Number of particles per ml} = \frac{N \times A_t}{n \times A_g \times V_f \times d}$$

where N = No. of particles counted (take N = 100 as an example)

A_t = Effective area of filter (area available for filtration of sample)

n = No. of grids counted (take n = 5 as an example)

A_g = Area of one counting grid

V_f = Volume filtered (take V_f = 350 ml)

d = Dilution factor (V final/V Sample)

$A_t = 0.7\ cm^2 = 7 \times 10^7\ \mu m^2$

@ 400x magnification, area of 1 counting grid = 250 μm x 250 μm = $6.25 \times 10^4\ \mu m^2$

$$\text{Number of particles per ml} = \frac{100 \times 7 \times 10^7}{5 \times 6.25 \times 10^4 \times 350 \times 1.11}$$

$$= 57.66 \text{ particles per ml}$$

@ 1000x magnification, area of 1 counting grid = 100 μm x 100 μm = $10^4\ \mu m^2$

$$\text{Number of particles per ml} = \frac{100 \times 7 \times 10^7}{5 \times 10^4 \times 350 \times 1.11}$$

$$= 360.4 \text{ particles per ml}$$

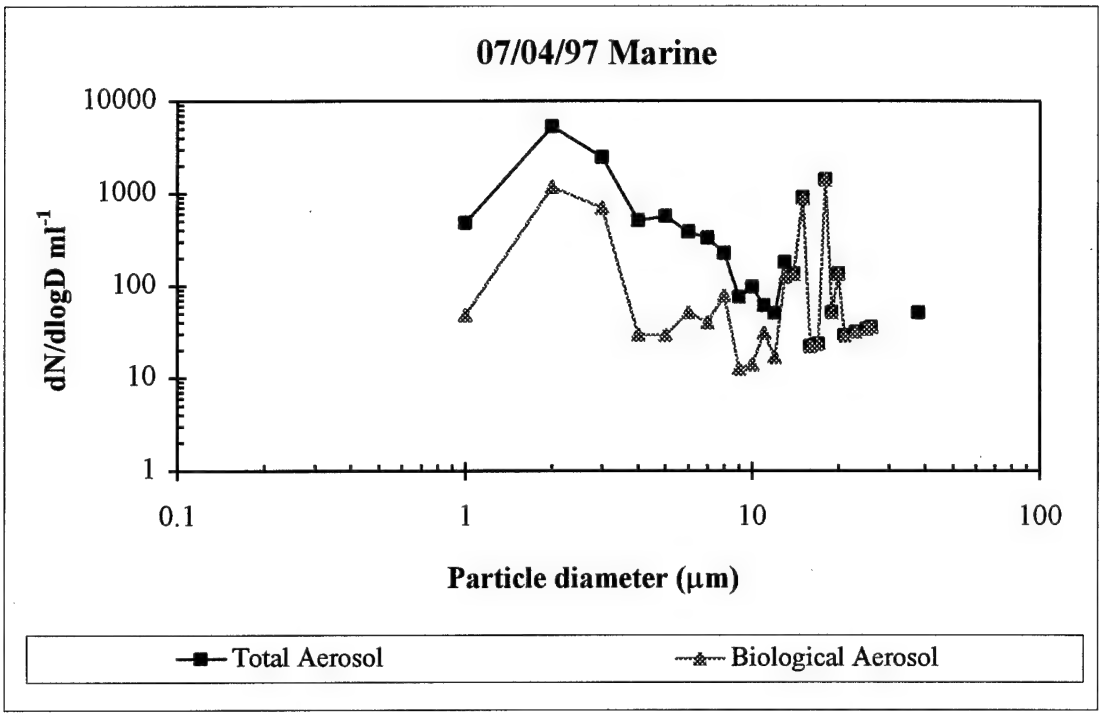

Figure 1 (a) Total and biological aerosol size distribution. dN/dlogD per ml vs. diameter (μm)

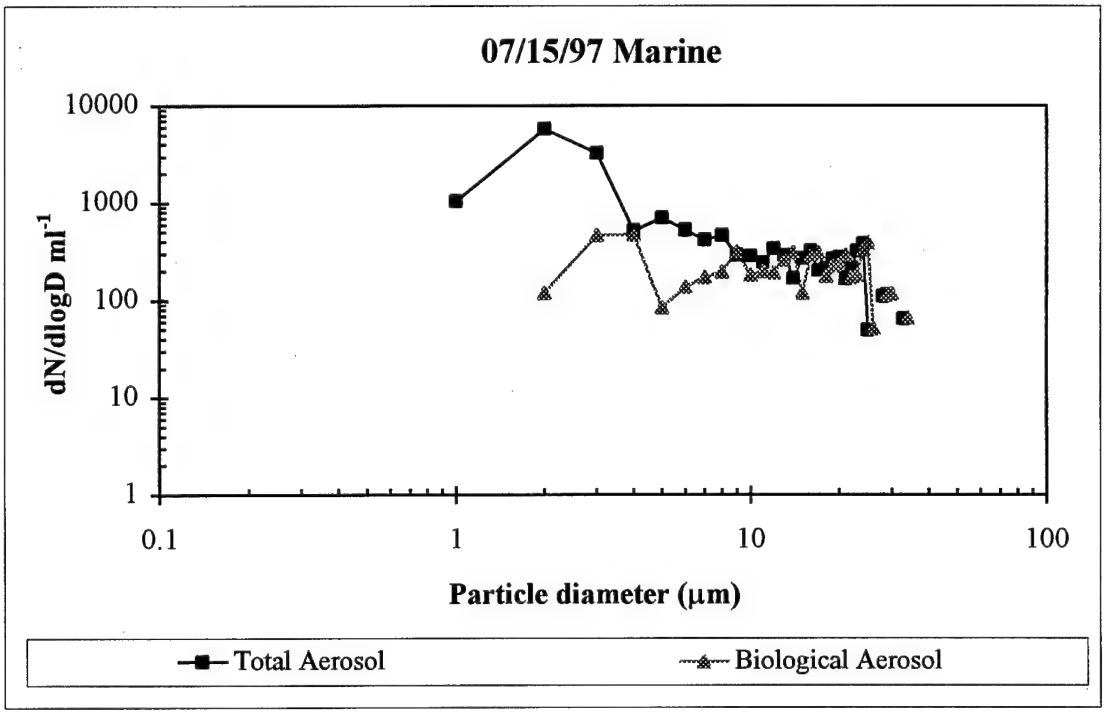

Figure 1 (b) Total and biological aerosol size distribution. dN/dlogD per ml vs. diameter (μm)

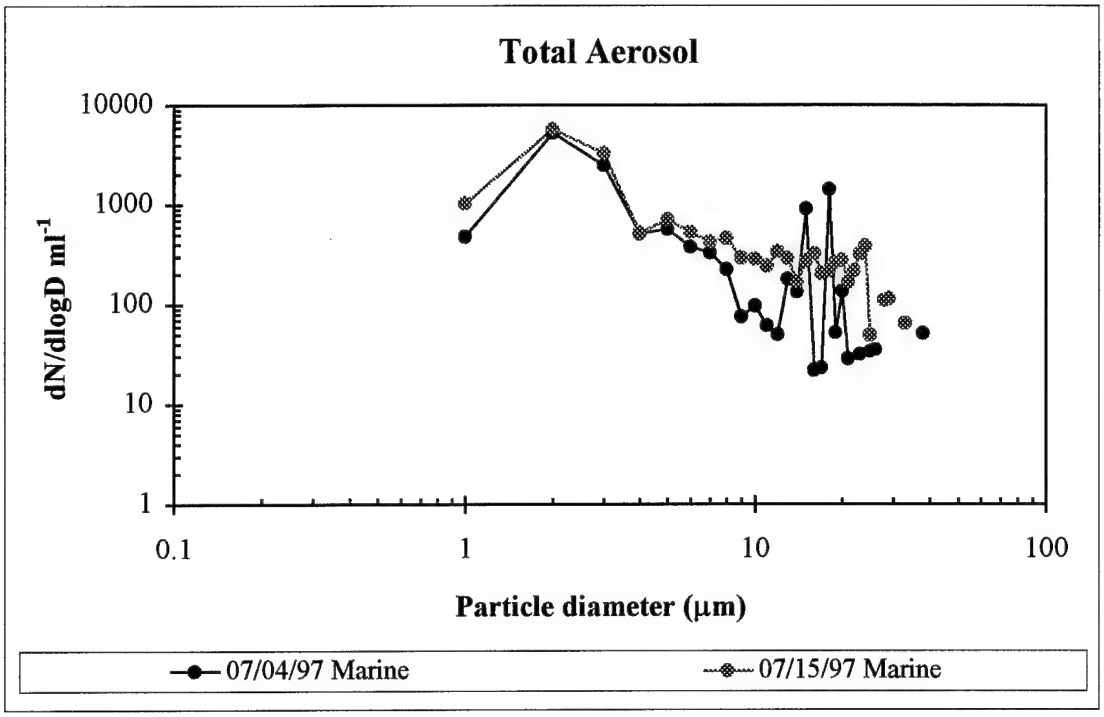

Figure 1 (c) Total aerosol size distribution. dN/dlogD per ml vs. diameter (μm)

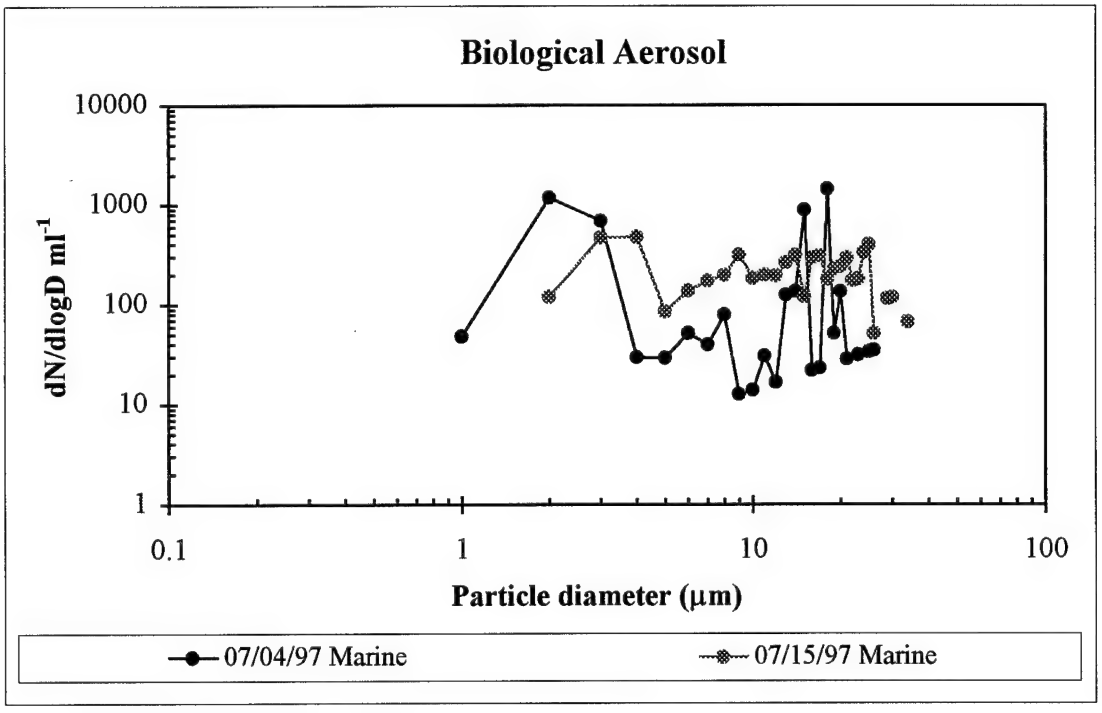

Figure 1 (d) Biological aerosol size distribution. dN/dlogD per ml vs. diameter (μm)

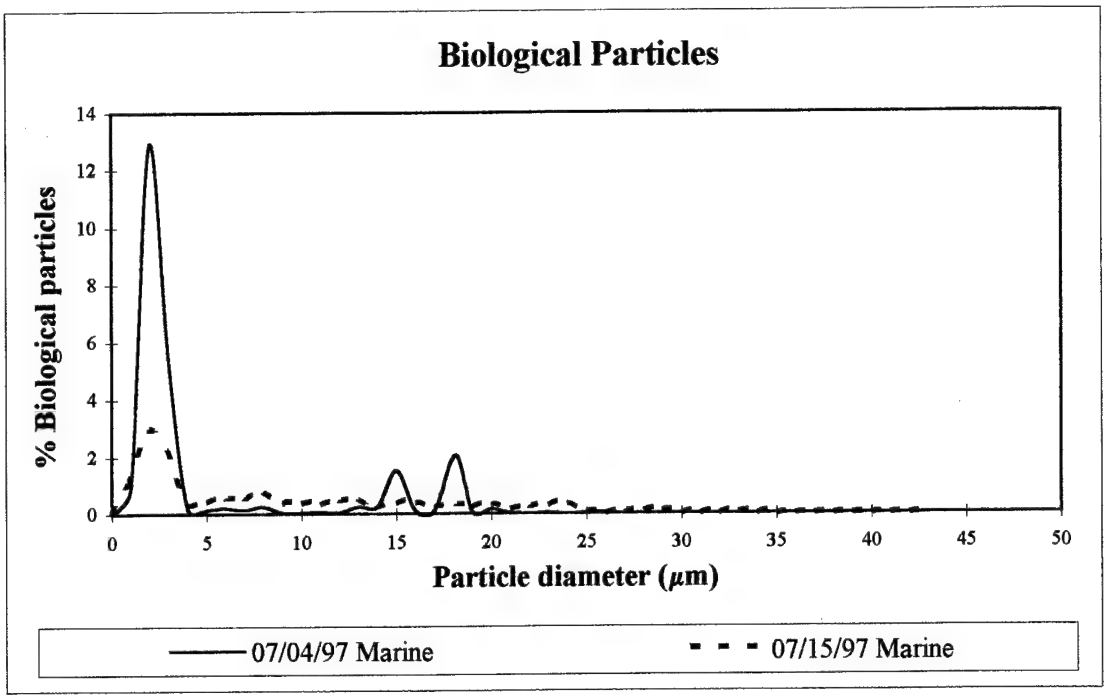

Figure 1 (e) Percentage (%) of biological particles to total aerosol particles vs. diameter (μm)

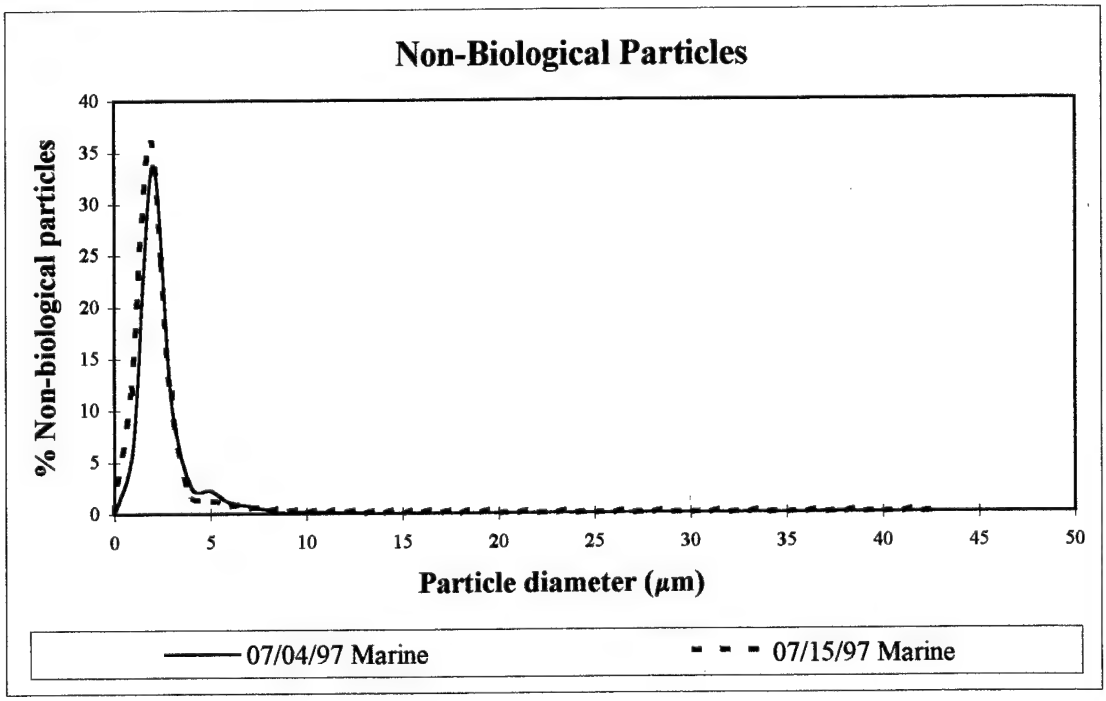

Figure 1 (f) Percentage (%) of non-biological particles to total aerosol particles vs. diameter (μm)

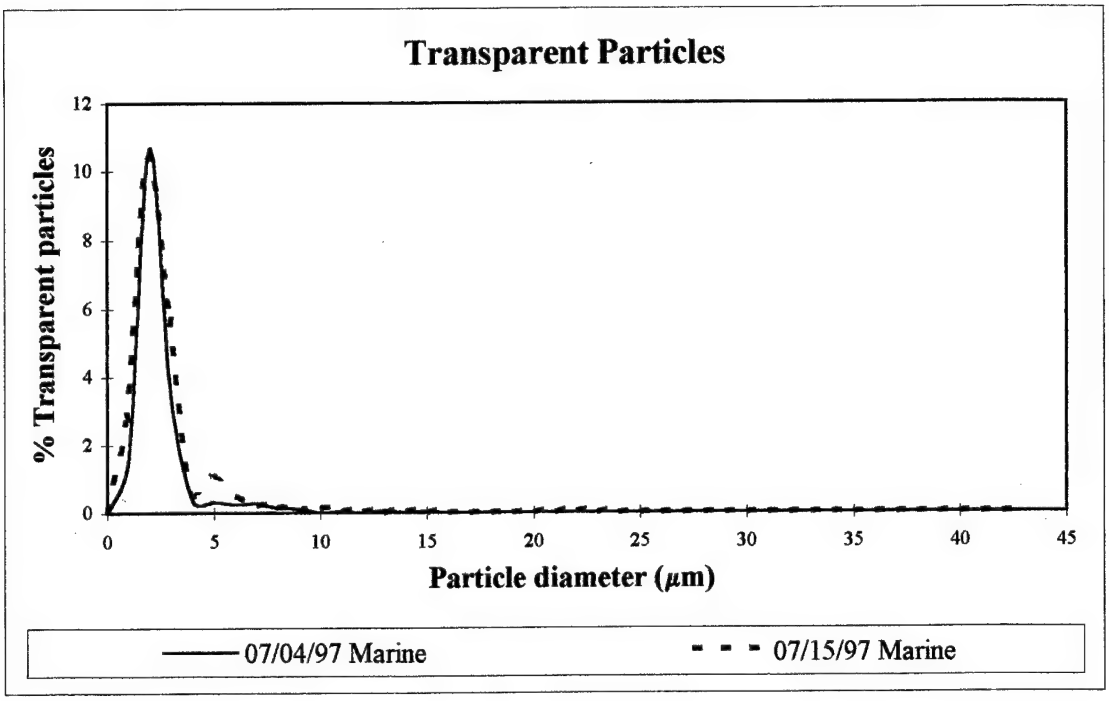

Figure 1 (g) Percentage (%) of transparent particles to total aerosol particles vs. diameter (μm)

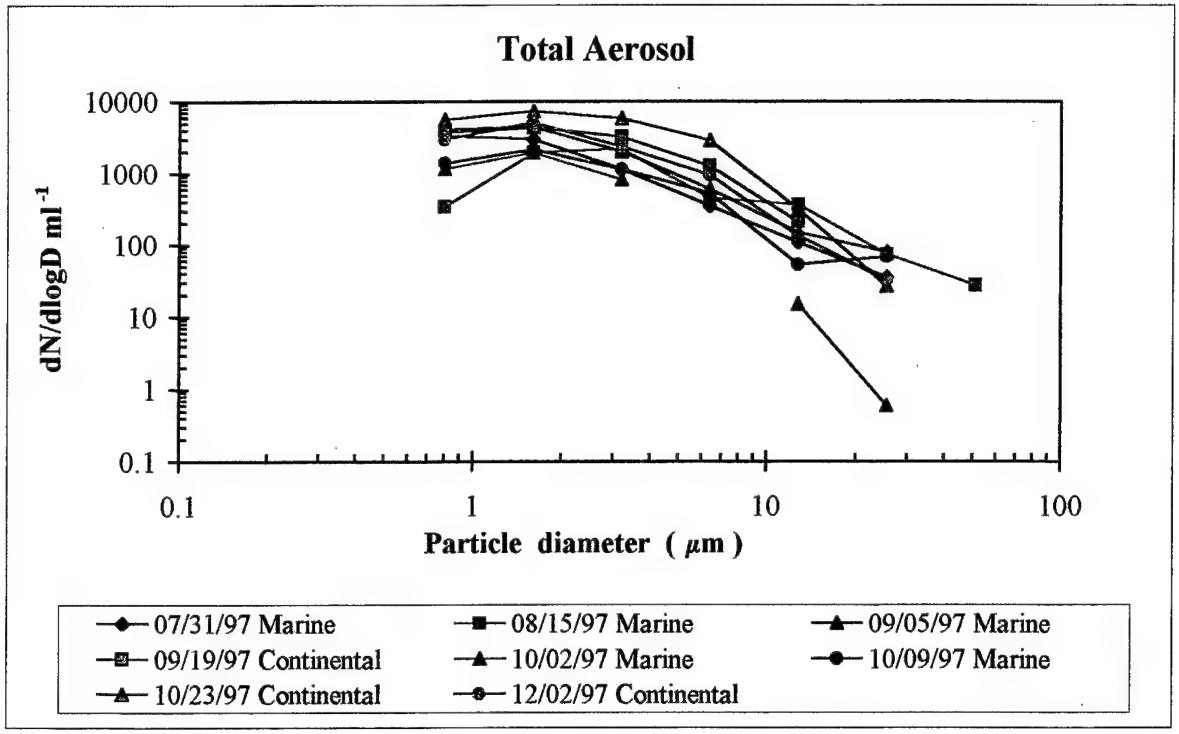

Figure 2 (a) Total aerosol size distribution. dN/dlogD per ml vs. diameter (μm)

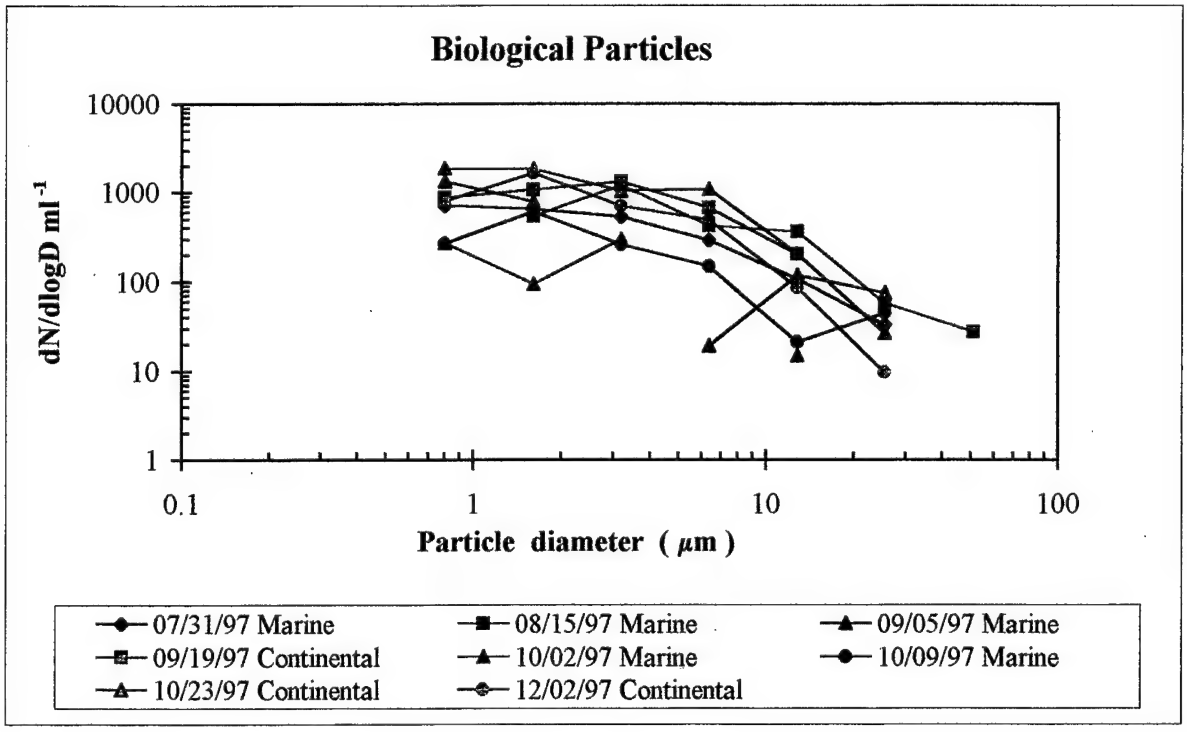

Figure 2 (b) Biological size distribution. dN/dlogD per ml vs. diameter (μm)

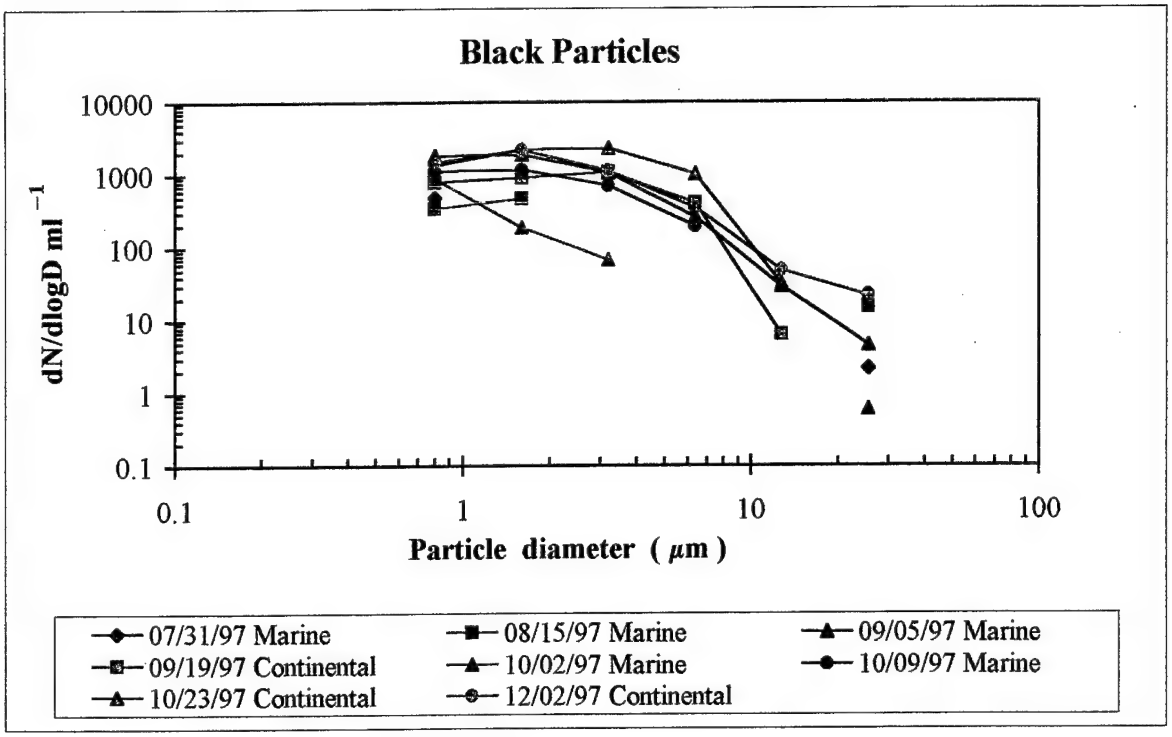

Figure 2 (c) Black particle size distribution. dN/dlogD per ml vs. diameter (μm)

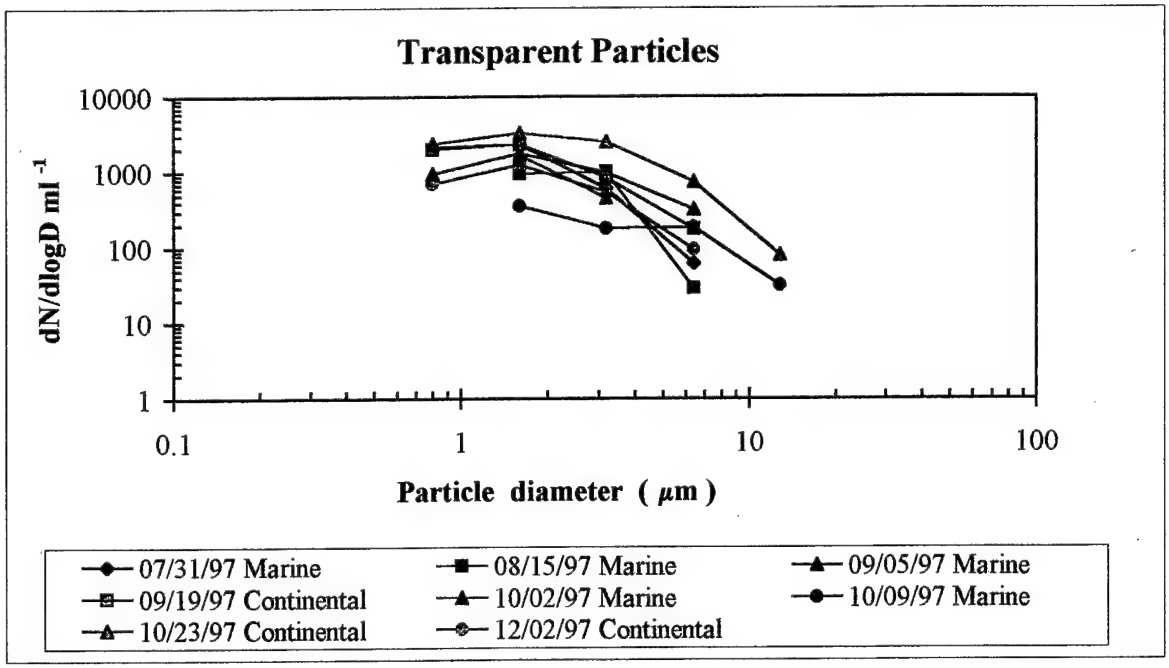

Figure 2 (d) Transparent particle size distribution. dN/dlogD per ml vs. diameter (μm)

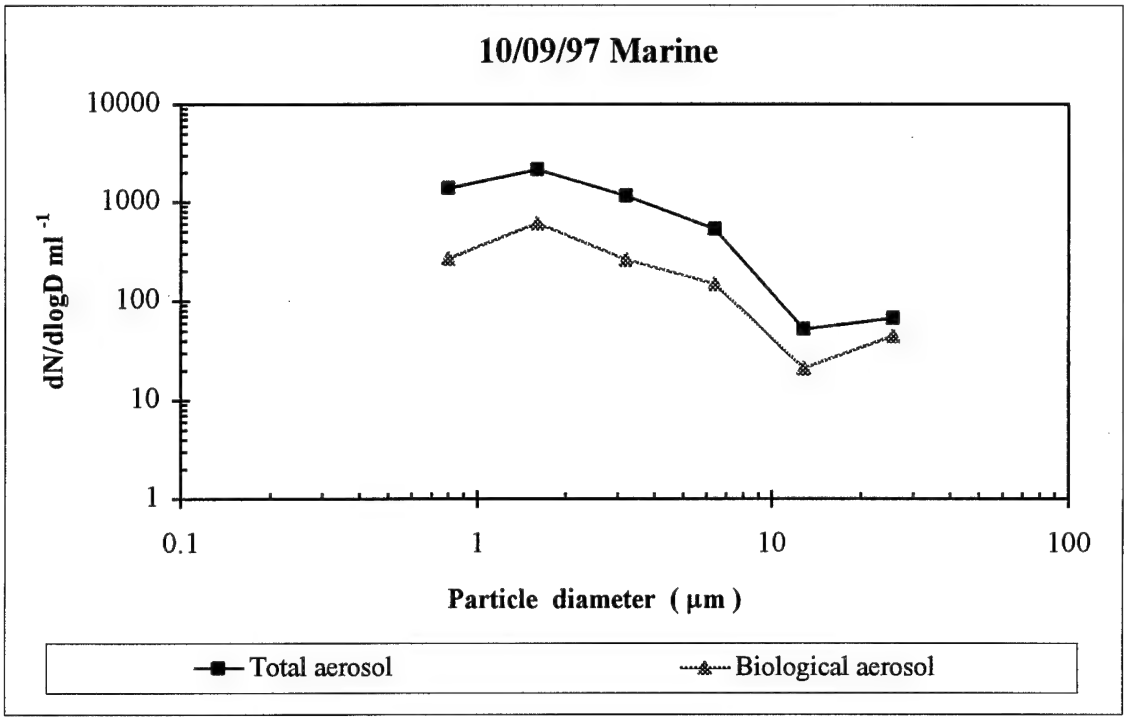

Figure 2 (e) Total and biological aerosol size distribution. dN/dlogD per ml vs. diameter (µm)

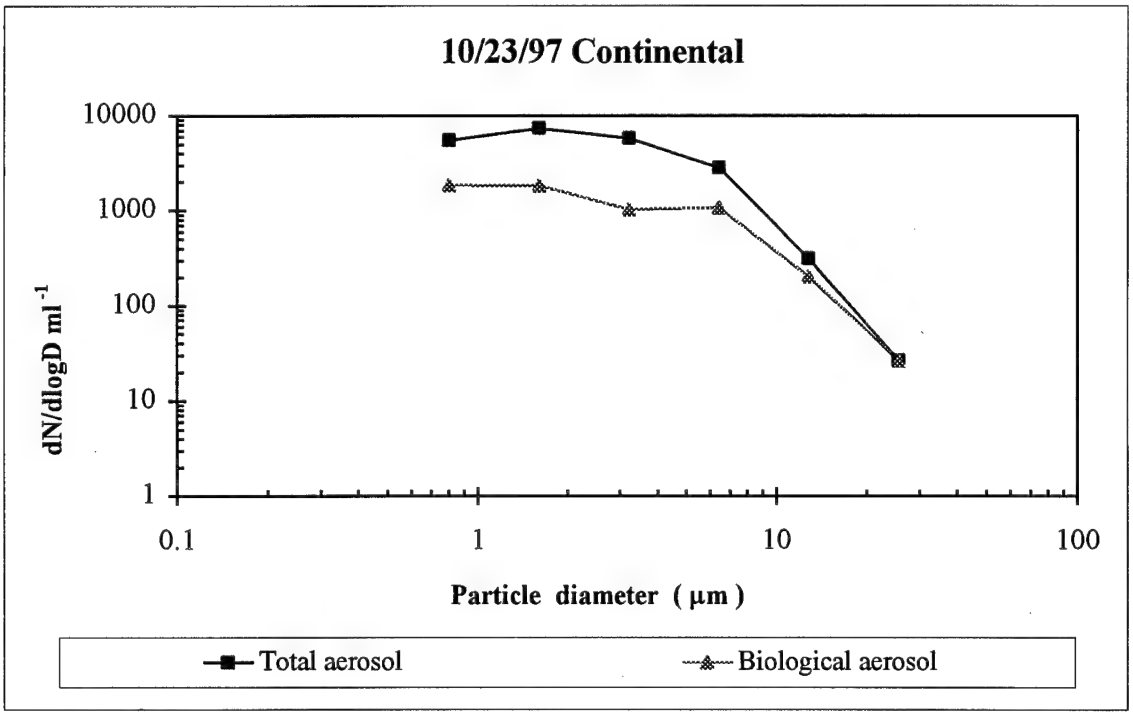

Figure 2 (f) Total and biological aerosol size distribution. dN/dlogD per ml vs. diameter (µm)

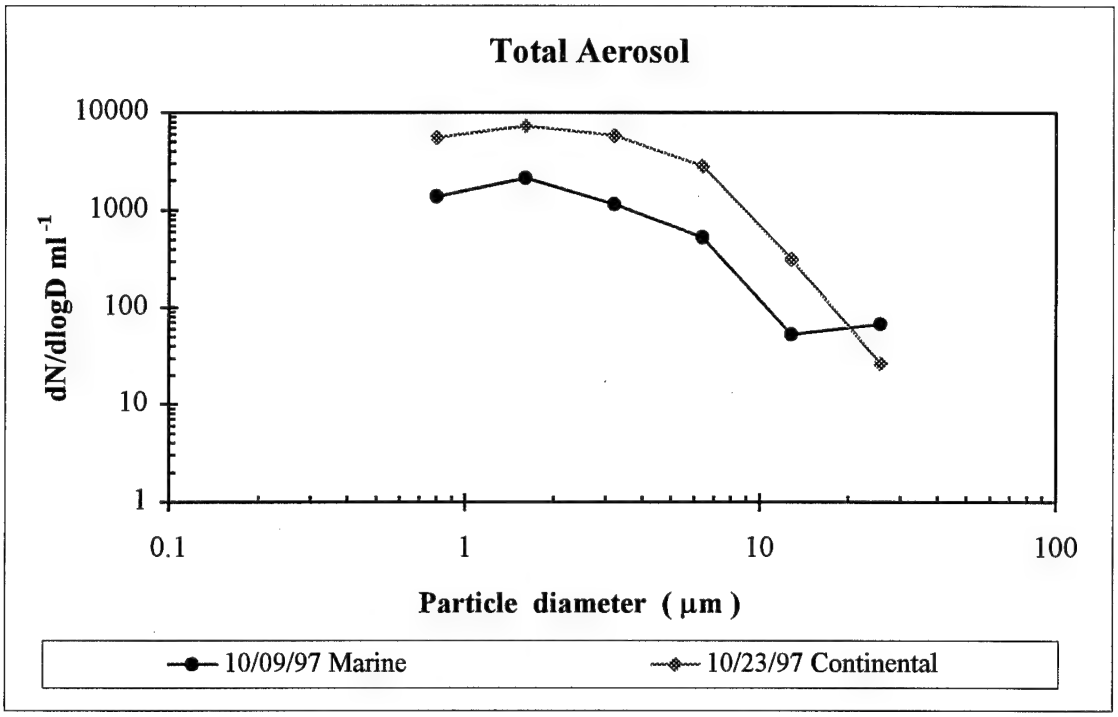

Figure 2 (g) Total aerosol size distribution. dN/dlogD per ml vs. diameter (μm)

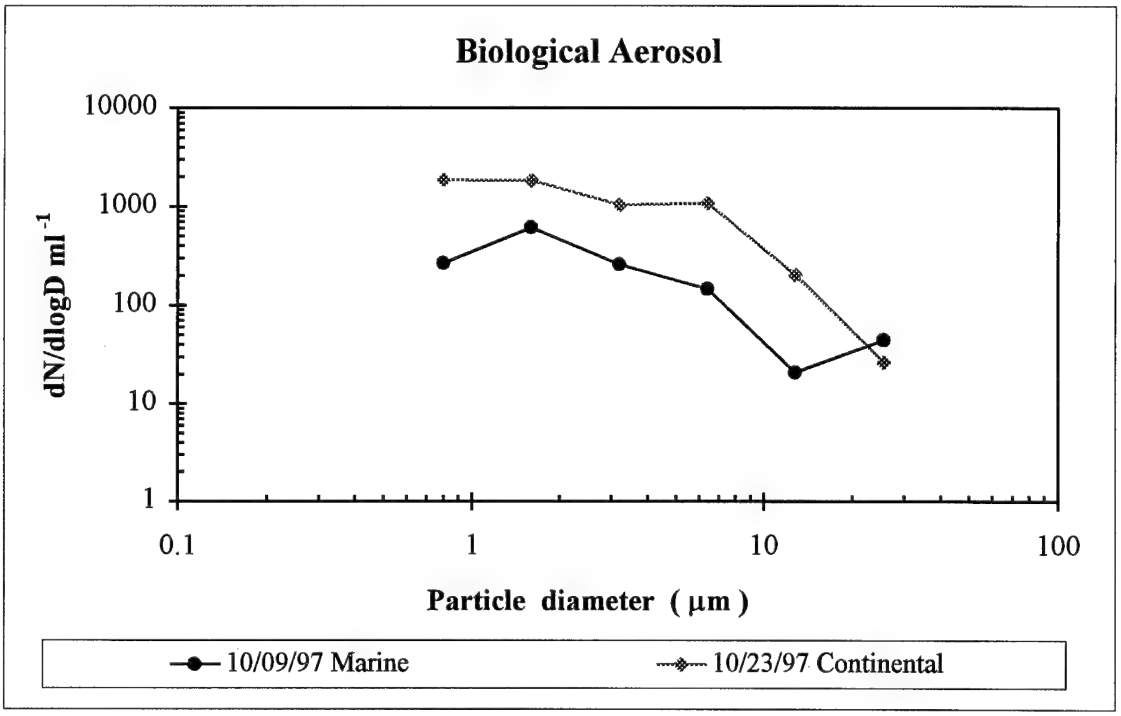

Figure 2 (h) Biological aerosol size distribution. dN/dlogD per ml vs. diameter (μm)

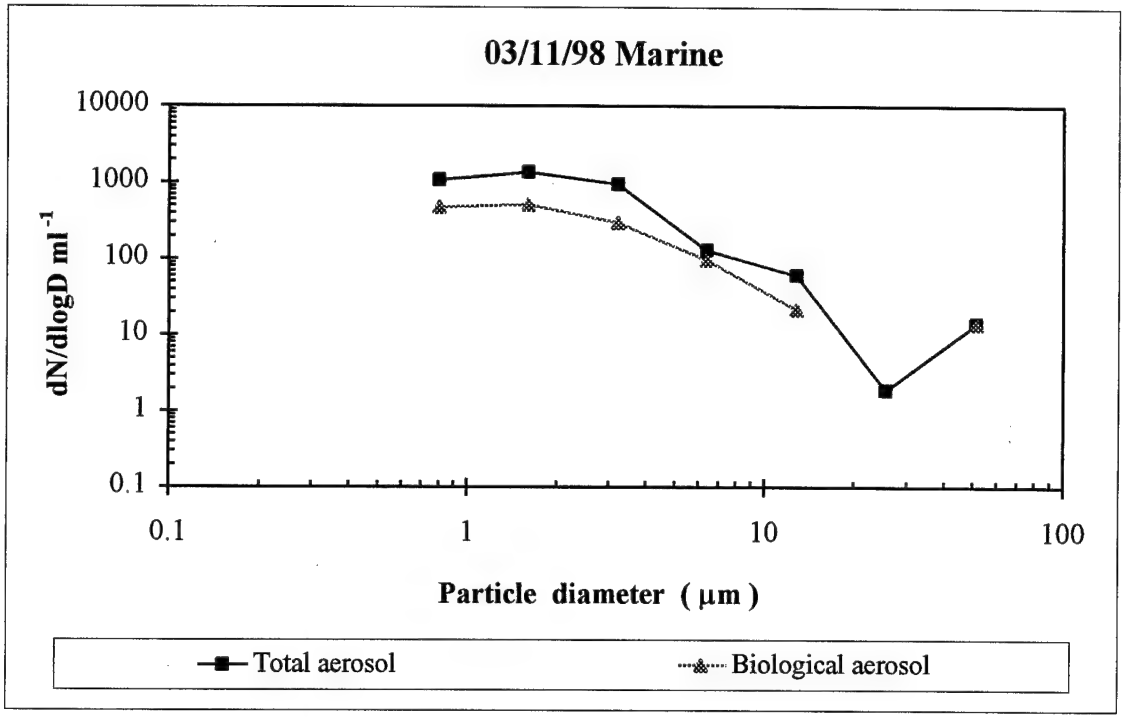

Figure 3 (a) Total and biological aerosol size distribution. dN/dlogD per ml vs. diameter (µm)

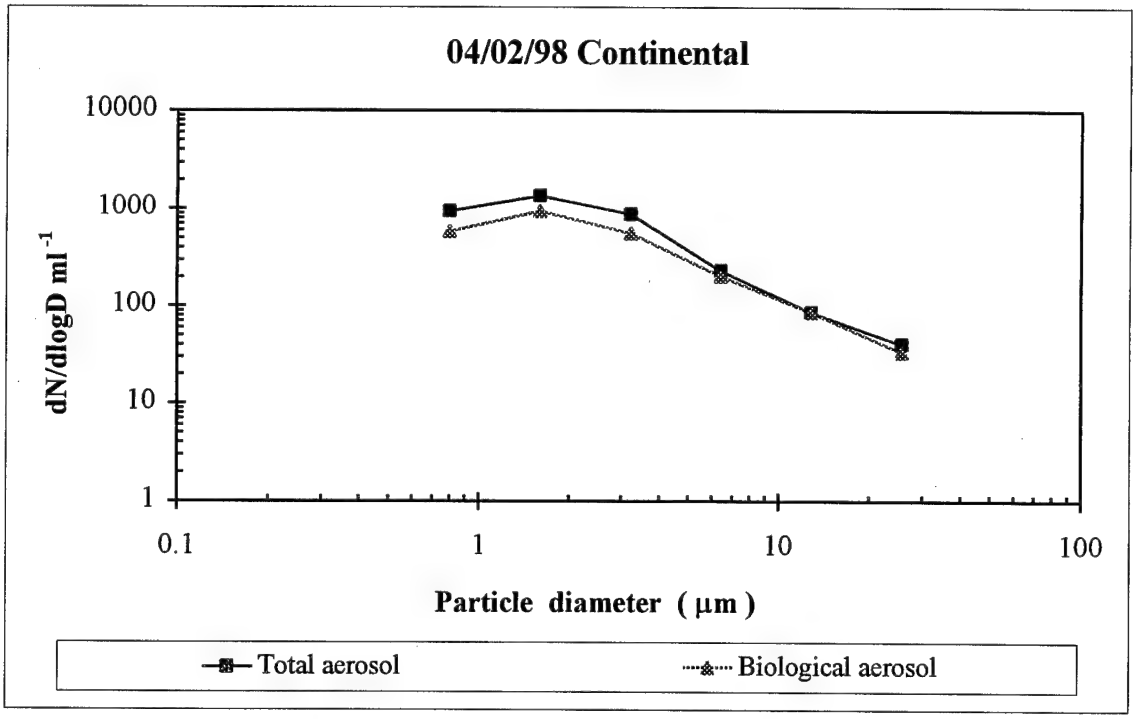

Figure 3 (b) Total and biological aerosol size distribution. dN/dlogD per ml vs. diameter (µm)

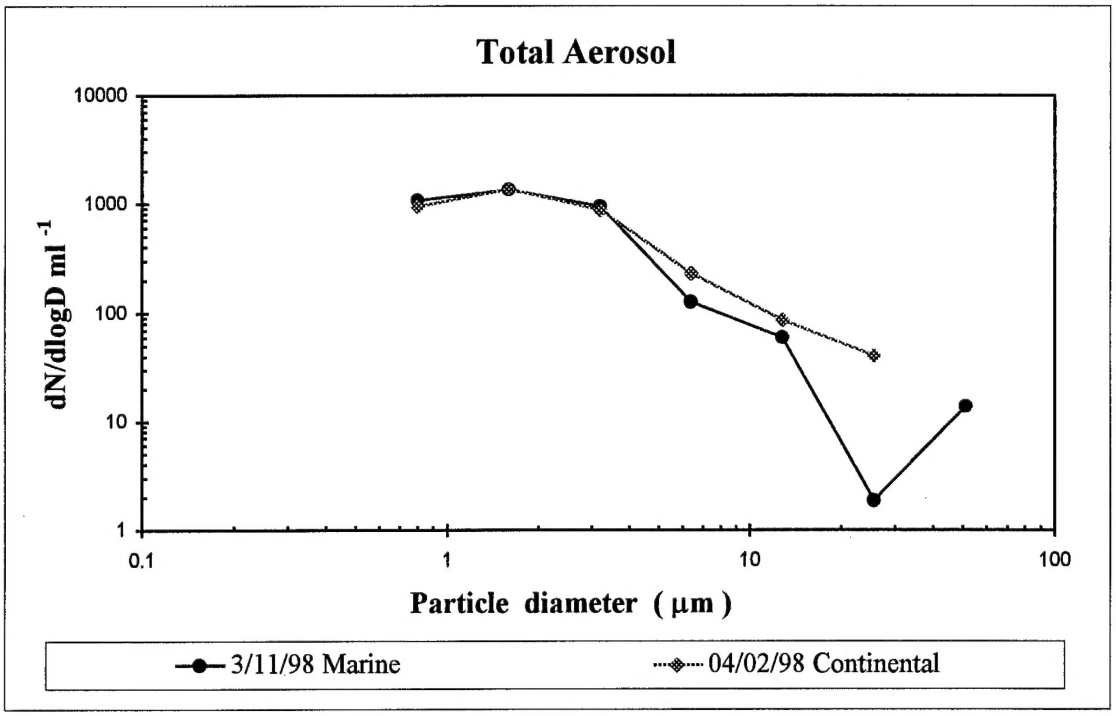

Figure 3 (c) Total aerosol size distribution. dN/dlogD per ml vs. diameter (µm)

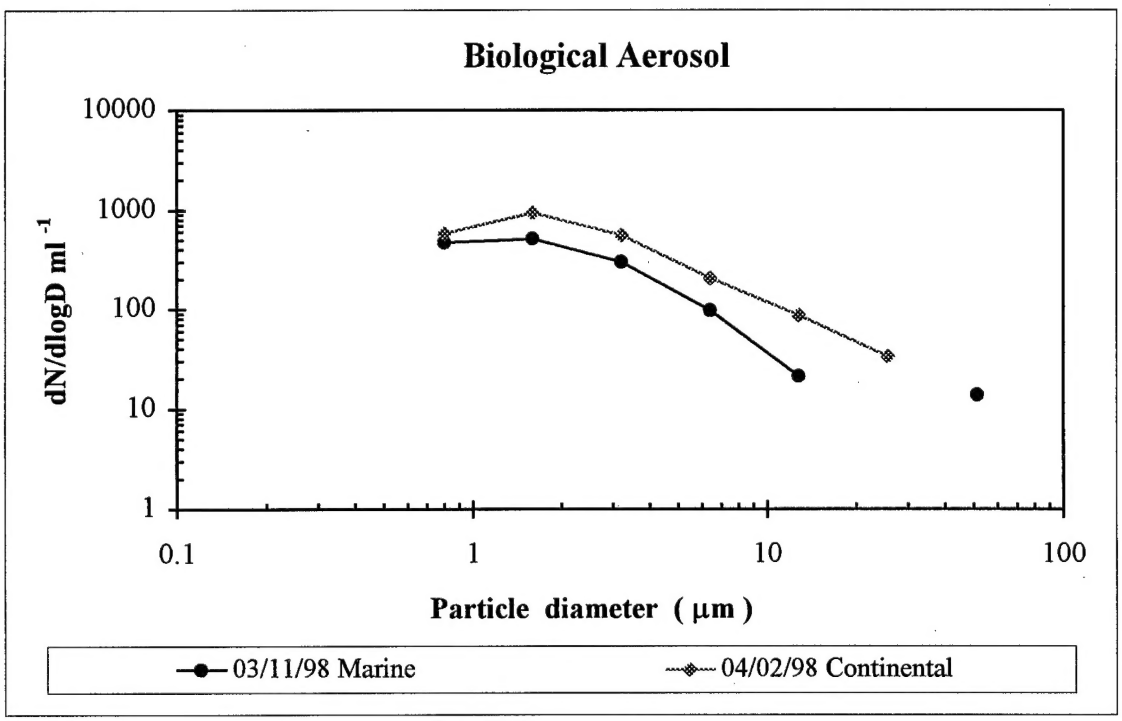

Figure 3 (d) Biological aerosol size distribution. dN/dlogD per ml vs. diameter (µm)

Figure 4 (a) 03/11/98 Marine

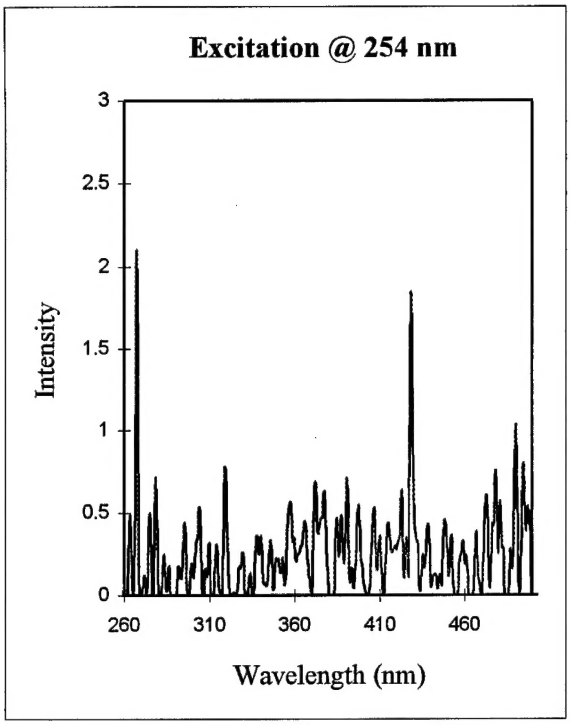

Figure 4 (b) 04/02/98 Continental

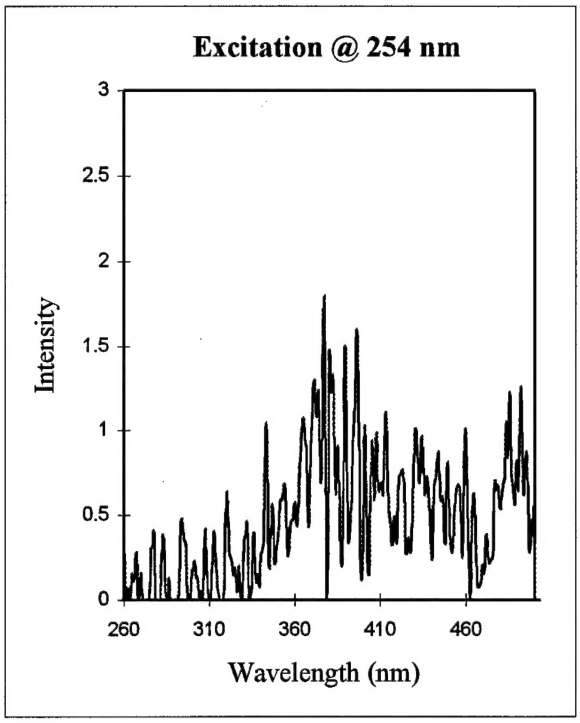

Figure 4 (c) 03/11/98 Marine

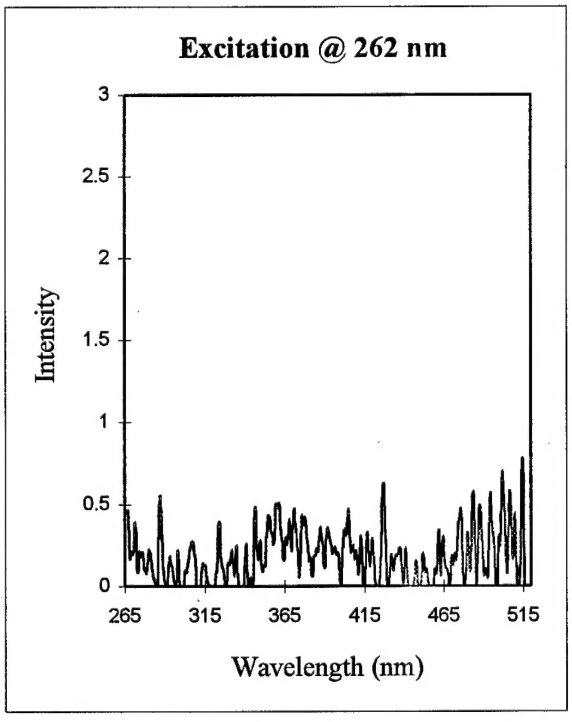

Figure 4 (d) 04/02/98 Continental

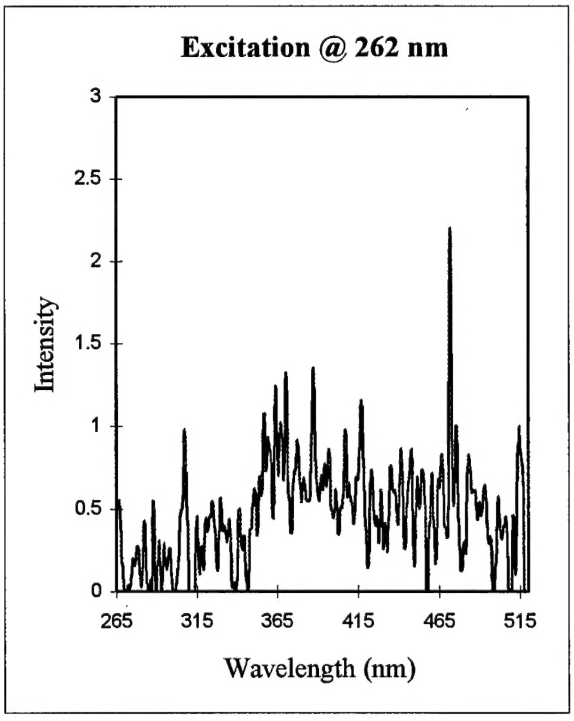

Figure 4 (e) 03/11/98 Marine

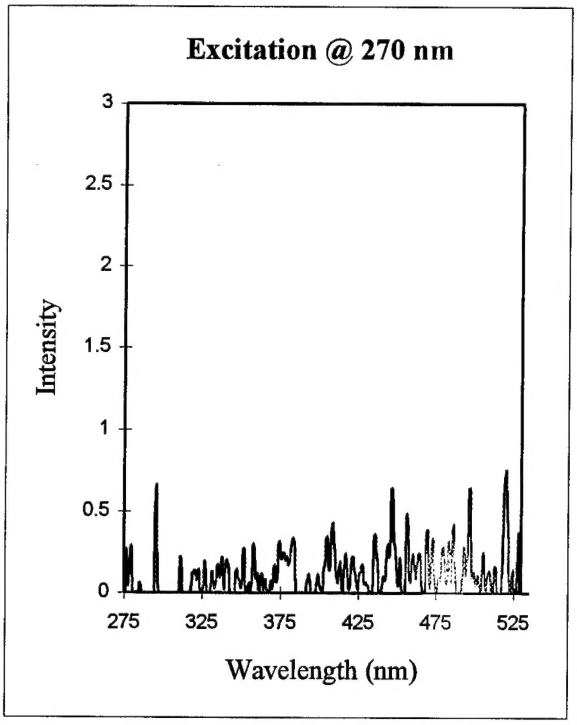

Figure 4 (f) 04/02/98 Continental

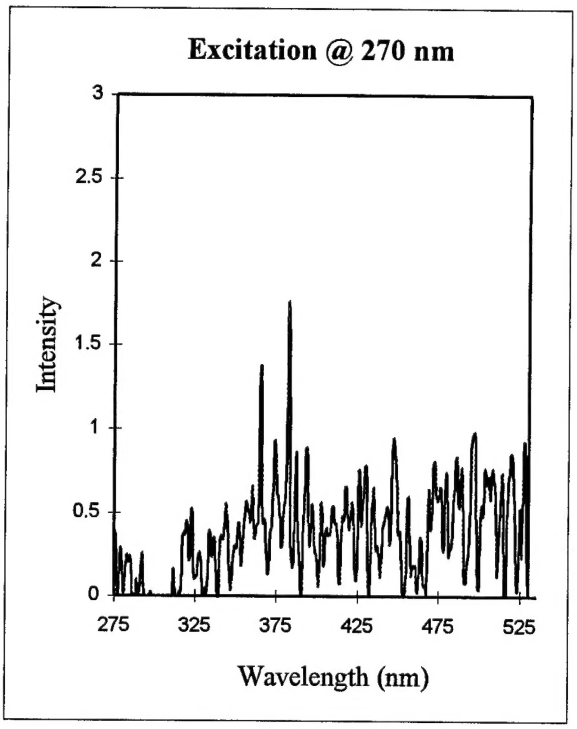

Figure 4 (g) 03/11/98 Marine

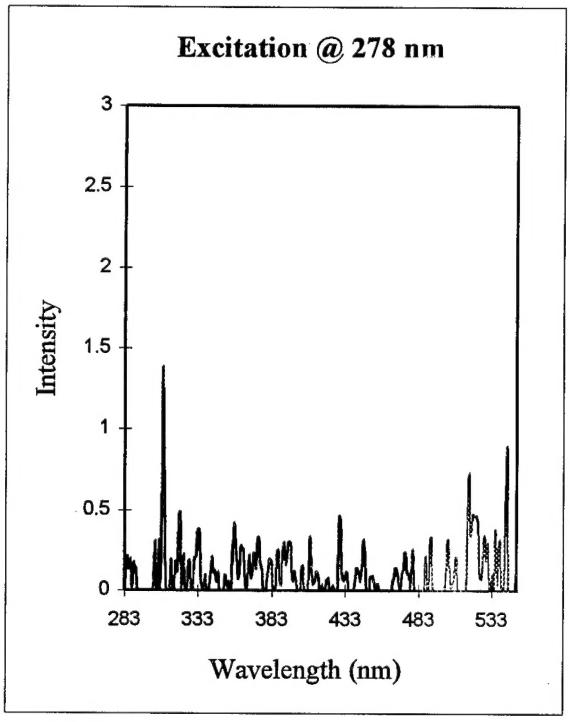

Figure 4 (h) 04/02/98 Continental

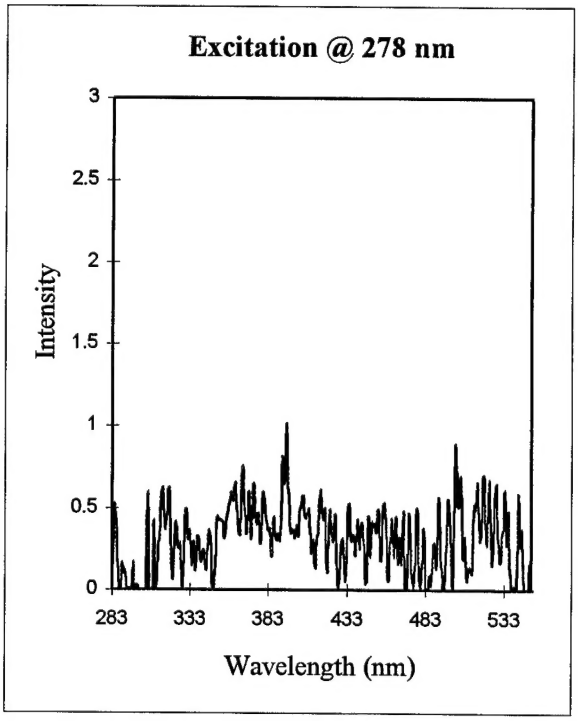

Figure 4 (i) 03/11/98 Marine

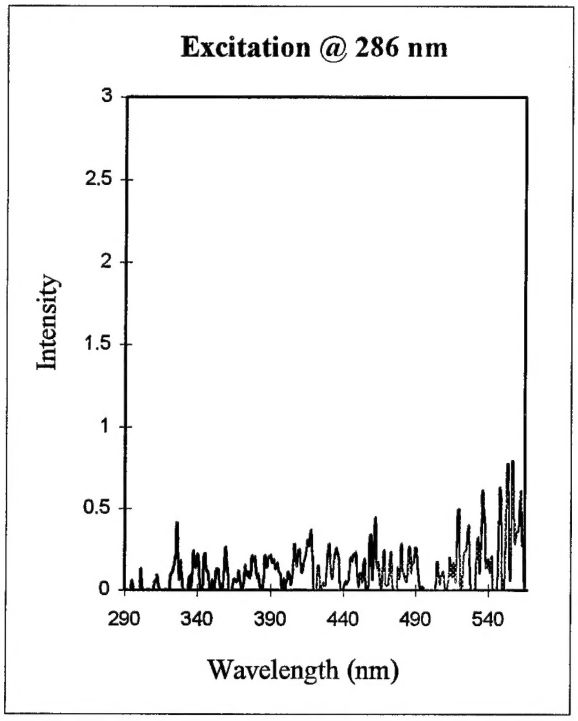

Figure 4 (j) 04/02/98 Continental

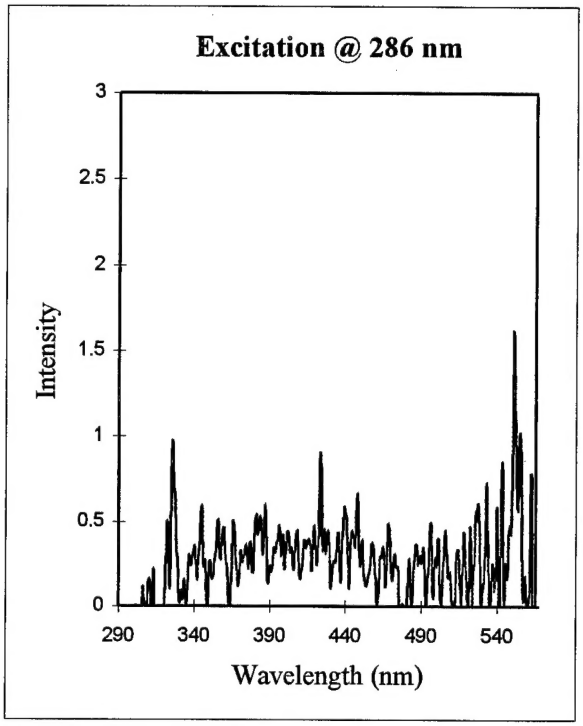

Figure 4 (k) 03/11/98 Marine

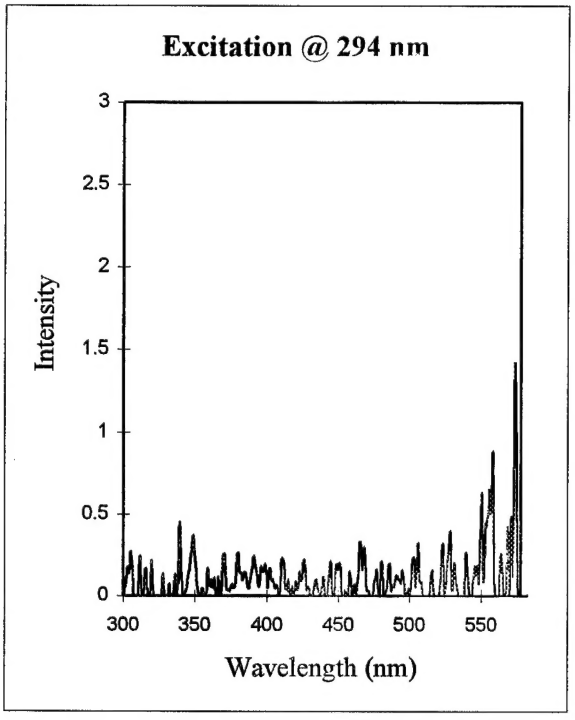

Figure 4 (l) 04/02/98 Continental